ISSN 0021-3640, JETP Letters, 2023, Vol. 118, No. 5, pp. 363–368. © The Author(s), 2023. This article is an open access publication.
ISSN 0021-3640, JETP Letters, 2023. © The Author(s), 2023. This article is an open access publication.

METHODS OF THEORETICAL PHYSICS

Metabolometer Based on Toroidal Response

M. Cojocari[a], A. Merenkov[a], F. Kovalev[a], S. Shitov[a,b], and A. Basharin[a,*]

[a] *National University of Science and Technology MISiS, Moscow, 119049 Russia*

[b] *Kotelnikov Institute of Radio Engineering and Electronics, Russian Academy of Sciences, Moscow, 125009 Russia*

**e-mail: alexey.basharin@gmail.com*

Received June 1, 2023; revised July 27, 2023; accepted July 27, 2023

Toroidal metamaterials stand out by extremely high-Q resonances. Their radiation losses are suppressed, and fields in the metamolecules are extremely high and sensitive to the additional losses. In this work, we introduce a novel concept of metabolometer. It is based on the combination of a microwave high-Q factor toroidal metamaterial as readout device with embedded micro-pad superconductor as an absorber of terahertz (THz) radiation. We establish that a pad with 20 kΩ/sq sheet resistance reduces metamaterial Q-factor and changes the stop-band level by as much as −50 dB at 1.5 GHz. Importantly, this sensitivity to the additional losses requires no galvanic connection to the absorber. This allows one to detect THz heating of superconducting pad via the change in metamaterial transmission spectrum. We consider the absorber as a superconducting hafnium film because of its nonlinear response at 1.5 GHz below $T_c = 400$ mK. Respectively, we estimate the losses in hafnium over temperature at the metamaterial resonant frequency using Mattis–Bardeen theory. This approach can significantly improve the future design of the terahertz/millimeter-wave detectors.

DOI: 10.1134/S0021364023601732

Metamaterials are artificial periodic structures with exceptional properties, unachievable in conventional electronic materials. Metamaterials can prevail as high Q-factor resonators in a wide frequency range [1–3]. Importantly, metamaterial devices can operate at low temperatures [4, 5]. Metamaterials can be manufactured in a single lithography step and their applications include harvesting devices, filters, and antennas [6]. This defines metamaterials as a promising platform for applications at high frequencies. Recently, a lot of work in this field is put into filling the THz frequency gap. Metamaterials cover all three devices of interest: sources [7], modulators [8–11], and detectors [12, 13] of THz radiation. The latter is the subject of this work.

THz detectors have applications in remote sensing [14], security applications [15], biomedicine [16, 17], and astronomy [18, 19]. There are several physical mechanisms THz detectors can work on. It can be based on the change in the properties of a material (surface charge, electrical inductance, resistance, and others) of a material, heated by THz radiation, or on electron transition induced by THz radiation [20]. Bolometers are one of the most widely used THz detectors. In general, bolometers are thermal detectors, which exploit materials with temperature-dependent electrical resistance. A bolometric thermometer is used to detect temperature rise of an absorber. The low-temperature operation (from several millikelvins to several kelvins) allows one to use a superconductor [21] for the bolometric thermometer. Superconductivity-based thermometer has an extremely sharp transition from zero resistance state to normal state. Such bolometers are called Transition Edge Sensor (TES) detectors [22]. They allow extremely sensitive measurement of the absorbed energy by measuring the temperature change of the absorbing pad. When the energy of the incoming photons exceeds the energy of the electron pairing, superconductor gains resistance that corresponds to its normal state. Then, the photon energy is converted into heat. Since Earth's atmosphere is low-transparent at terahertz frequencies, superconductor absorbers are promising for space applications. Importantly, Planck's spectrum of the Cosmic Microwave Background has a roll-off above 1 THz. This makes Outer Space transparent for it, allowing observation of the most distant regions of the Universe using the highest sensitive detectors, primarily the superconducting bolometers. The astronomical community imposes high requirements on the detector characteristics due to extremely low signal levels available from the Cosmic Microwave Background Radiation [18, 23] and other objects of the Deep Space [24].

Metamaterials with easy-to-engineer properties have been of significant use in the development of devices that meet these requirements. Metamaterials are usually integrated into bolometers as absorbers [25, 26]. As a result, one can broaden [27], narrow [13]

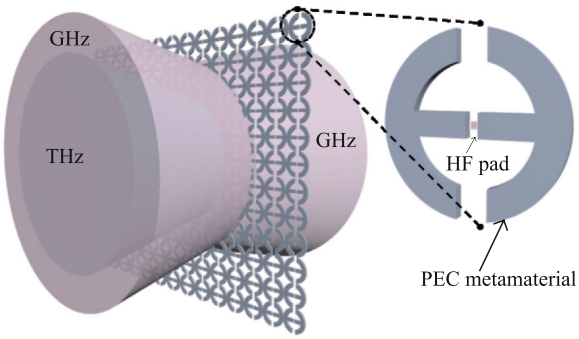

Fig. 1. (Color online) Metamaterial design. External radius of the metamolecule is 52.5 mm; lateral gaps are 6.3 mm wide and central gap is 4.2 mm, thickness of the sheet PEC is 0.2 mm. Hafnium absorbers in the center of each metamolecule are 0.5 × 0.5 mm (shown in the inset). GHz beam excites resonance in the metamaterials, while THz beam changes the state of the absorbing Hf pads placed in the center of each metamolecule.

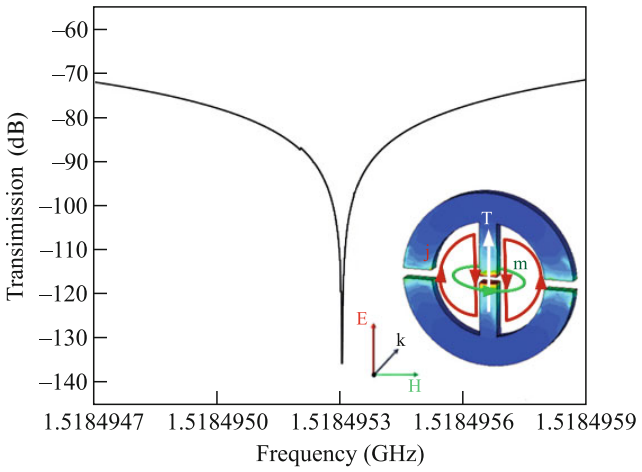

Fig. 2. (Color online) Simulated transmission spectrum. The inset depicts the distribution of the electric field. The red color in the center of the metamolecule corresponds to maximum of the electric field (27070 V/m).

or move the bandwidth, increase sensitivity, and control the speed of operation [28].

In this work, we propose a metabolometer based on high Q-factor microwave toroidal metamaterial with integrated absorbing superconducting pad (Fig. 1). The resistance of superconducting elements can be varied by absorption of THz radiation (heating), which drastically changes the metamaterial microwave response. We study numerically the dependence of metamaterial resonance characteristics on the resistance (R) of the absorber pad. To explain the nonlinear spectral feature, we perform multipole expansion of the response at the resonance frequency for different values of R. We also estimate theoretically how characteristics of the resonance change over the pad temperature in the case of the square-shaped absorber made from a superconducting hafnium film.

The metamaterial we choose to play the role of the high Q-factor resonator is anapole metamaterial proposed by Basharin et al. [29]. Its outstanding properties have been used to benefit such devices as THz modulators and resonators by authors [30, 31] and other teams [32, 33], as demonstrated by the authors. Among the properties of chosen metamaterial, we highlight the negligible impact of the losses in real conductors on the metamaterial Q-factor: just two orders of magnitude less [29]. The array of metamolecules was simulated with periodic boundary conditions. Each of the periodically arranged metamolecules consists of two mirrored epsilon letters as shown in Fig. 1. In the simulation, an incident microwave radiation, polarized along the central wires, penetrates the single PEC metamolecule accounting for the periodic boundary conditions of their array. It excites two counter directed currents in the metamolecule voids, which results in magnetic fields vectors being rotated around the central strips (inset in Fig. 2). Such field configuration resembles a torus cross section, which enables excitation of the toroidal dipole moment along with the electric dipole moment. We start by evaluating and tuning the properties of the metamaterials without the absorber. The dimensions of a metamolecule are chosen so that the transmission spectrum (Fig. 2) exploits a deep resonance at 1.5185 GHz. The minimum of transmission reaches 130 dB. The inset in Fig. 2 shows that the electric field is localized in the central gap of the metamolecule at the resonance frequency.

Correspondingly, we incorporate an absorbing (Hf) pad between the central strips, 1.85 mm away from each (Fig. 1). We study, then, how the metamaterial resonance from Fig. 2 changes with the increasing resistance of the pad. The role of the absorber plays a 0.5 × 0.5 mm pad with variable surface resistance. Physically, this means that bolometer based on our metamaterial is illuminated with two electromagnetic waves at the same time. The wide microwave beam is the plane wave at the resonance frequency of the metamaterial. The second beam is THz radiation which is absorbed by a lossy element (Hf pad) in the center of each metamolecule. They are depicted as pink and blue beams in Fig. 1 correspondingly.

While simulating nonlinear Hf absorber, we consider the model of its high-frequency-induced transition from superconducting to the normal state. We plot its resonance minimum over the surface resistance of the pad in Fig. 3. The actual transmission spectra for small resistance varying from $R = 55$ Ω/sq to $R = 160$ Ω/sq are presented in the inset in Fig. 3. We observe a resonance frequency shift in Fig. 3 in comparison to Fig. 2 because the presence of the absorber (the piece of metal) slightly changes the capacitance of the metamolecule. For the resistance

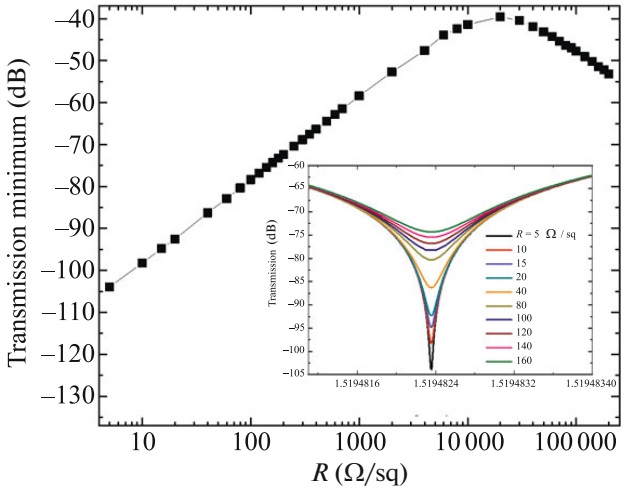

Fig. 3. (Color online) Transmission minimum versus the resistance of the inserted absorber. (Inset) Simulated transmission spectra for different resistance of the insertion.

up to 160 Ω/sq, simulations predict no essential change of the resonance frequency, though the Q-factor is strongly reduced. For the larger resistance, resonance frequencies change slightly (about 3×10^{-3}). The resistance dependence of the transmission minimum demonstrates a maximum at $R = 10$–20 kΩ/sq as shown in Fig. 3. This maximum corresponds to the matching point of the effective resistance of the absorber and the active part of the resistance of the electromagnetic field in the toroidal resonator. The absorber in the matching condition can dissipate the maximum of the power from the resonator, thus reducing the toroidal effect to its minimum. The reference level at the matching point is about –40 dB.

To explain the nonlinearity of the resonance characteristics over pad resistance, we perform multipole expansion of the currents excited in each metamolecule for different values of R. Along with electric dipole moment $\mathbf{P}$, we consider the following multipoles (Fig. 4a): magnetic dipole, $\mathbf{M}$, and toroidal dipole, $\mathbf{T}$, moments and electric, $\mathbf{Q}_e$, and magnetic, $\mathbf{Q}_m$, quadrupoles. We also add the multipoles of the next order, i.e., mean-square radii of toroidal $\mathbf{R}_T$ dipole and magnetic quadrupole $\mathbf{R}_{Qm}$, to the expansion [34, 35]. Since other multipoles of mean-square radii are close to zero, we do not show them in Fig. 4. Although radiation intensity of mean square radii multipoles is low, for the correct characterization of the system, their contributions must be considered.

The metamaterial resonance is determined by toroidal dipole moment, accompanied by electric dipole and magnetic quadrupole moments. Up to 10 kΩ/sq, the difference between electric and toroidal multipoles is increasing, ruining the anapole state and

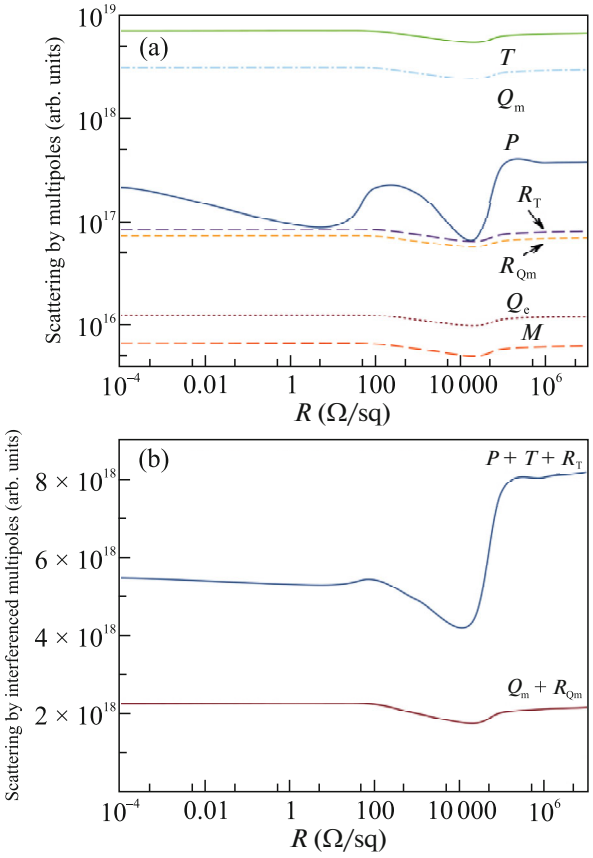

Fig. 4. (Color online) Scattering by multipoles (a) and interference multipoles (b) at resonance frequency versus pad surface resistance.

decreasing the resonance depth (Fig. 4). At 10–20 kΩ/sq, the difference between electrical and toroidal dipole is maximal. It causes the biggest deviation from the anapole state, and the resonance amplitude achieves its minimal value (see Fig. 3). To investigate these multipoles' interaction, we study the scattering by the interfered multipoles (Fig. 4b). As expected, the interaction between toroidal and electric dipoles (considering the contribution of toroidal mean-square radius) experiences a minimum at 10–20 kΩ/sq. At the higher values of R, the scattering by interfered T and P increases as the resonance is getting deeper (Fig. 3).

In the actual structure, the superconducting hafnium film can be considered as a promising yet easy-to-use candidate for the role of bolometer absorber. Physically, the resistance of hafnium film in high-frequencies can be explained using the Mattis–Bardin theory [36] with the following equations:

$$\frac{R}{R_N} = \frac{\sigma_1 \sigma_n}{\sigma_1^2 \sigma_2^2}, \quad (1)$$

$$\frac{\sigma_1}{\sigma_n} = \frac{2}{\hbar\omega}\int_{\Delta(T)}^{\infty}(f(u)-f(u+\hbar\omega))g(u)du + \frac{1}{\hbar\omega}\int_{\Delta(T)-\hbar\omega}^{-\Delta(T)}(1-2f(u+\hbar\omega))g(u)du, \quad (2)$$

$$\frac{\sigma_2}{\sigma_n} = \frac{1}{\hbar\omega}\int_{\Delta(T)-\hbar\omega-\Delta(T)}^{\Delta(T)}(1-2f(u+\hbar\omega))g'(u)du, \quad (3)$$

$$g(u) = \frac{u^2+\Delta(T)^2+\hbar\omega u}{\sqrt{u^2-\Delta(T)^2}\sqrt{(u+\hbar\omega)^2-\Delta(T)^2}}, \quad (4)$$

$$g'(u) = \frac{u^2+\Delta(T)^2+\hbar\omega u}{\sqrt{\Delta(T)^2-u^2}\sqrt{(u+\hbar\omega)^2-\Delta(T)^2}}, \quad (5)$$

where R/R_N is the normalized resistance, $f(u)$ is the Fermi–Dirac function, $\Delta(T)$ is the temperature-dependent energy gap, σ_1 and σ_2 are the real and imaginary parts of the complex conductivity of the superconducting state ($\sigma = \sigma_1 + i\sigma_2$), and σ_n is the normal conductivity.

We use Eq. (1)–(5) to plot the temperature dependence of hafnium resistance at 1.5 GHz (Fig. 5, red). Hafnium, despite its potential as a material of interest, remains underexplored and less popular in current research endeavors. In our simulations, we use the hafnium film properties reported in the following papers [37–41]. Closer to the critical temperature $T_c = 0.375$ K the superconducting phase transition occurs in magnetron sputtered at a direct current hafnium with thicknesses up to 60 nm. The receiving system in our setup is set to be the hafnium film. Heated by THz radiation it changes the GHz response of the metamaterial. Metamaterial is designed to have resonance in GHz frequency range due to two main reasons. First, we work with the metamaterial with a sharp resonance with high Q-factor. This allows us to achieve the sensitivity reported in the paper. The detection of such a high Q-factor resonance in the THz frequency range has proven itself to be a challenging task in metabolometer applications [42–44]. Second, the superconducting hafnium film used as the absorber has a nonlinear response at 1.5 GHz below $T_c = 400°C$. Thereafter, the nonlinear response is possible below its critical temperature. We use this data to estimate the dependence of the response of the proposed bolometer on the temperature of hafnium pad heated by THz radiation (Fig. 5, gray), using the correspondence of transmission minimum of metamaterial and pad resistance from the Fig. 3. A strong correlation between the resistance of the hafnium predicted by Mattis–Bardeen theory and transmission of the metamaterial can be observed when comparing red and gray curves in Fig. 5.

Indeed, the concept of metabolometer can be exploited as extremely sensitive sensor of external radiation by the following. The heating of the Hf pad induced by THz radiation can be detected by corresponding changes in metamaterial transmission microwave spectrum. For example, the transmission level –60 dB would correspond to 0.37 K (Fig. 5). Moreover, the insignificant temperature change of 0.01 K gives rise to the substantial change (up to 7 dB) of the transmission level: from –67 to –60 dB. Such properties of the metabolometer make it a promising platform for hybrid astronomy detector of low THz radiation. We note that metamaterial component is purely metal, and our approach requires a superconductor only for a micro-pad absorber.

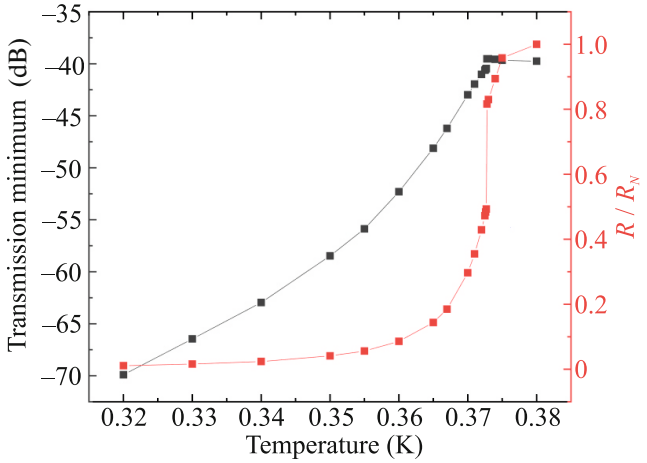

Fig. 5. (Color online) (red) Normalized resistance estimated by Mattis–Bardeen theory for hafnium and (grey) the transmission minimum from Fig. 3 versus the temperature of the hafnium absorber near its critical temperature.

In conclusion, we proposed a model of a superconducting metabolometer. We demonstrated that toroidal metamaterials are very promising candidates for bolometers applications due to strongly localized electric fields and extremely high Q-factor transmission spectra. This allows toroidal metamaterials to detect the slightest change of incorporated absorbers resistance. The proposed bolometer is based on the superconducting transition. To show this, we used Mattis-Bardeen theory to evaluate the dependence of the metamaterial resonance characteristics on the temperature of Hf pad. In the practical implementation, a focused THz beam would heat the absorber, while a plane GHz wave would be used for reading the absorber's temperature at the resonant frequency of the toroidal metamaterial. The depth of the resonance on the transmission spectrum of the GHz wave would reveal the temperature of the pad, and, correspondingly, the frequency of the detected THz radiation. Practical realization of the proposed bolometer has potential applications in astronomy as detectors of extremely low THz signal levels available from the

Cosmic Microwave Background Radiation [15, 19] and other objects of the Deep Space [20].

FUNDING

This work was supported by the Ministry of Education of the Russian Federation (project no. K2-2018-015) and by the Ministry of Science and Higher Education of the Russian Federation (strategic project Quantum Internet, program of strategic academic leadership Priority 2030).

CONFLICT OF INTEREST

The authors declare that they have no conflicts of interest.

REFERENCES

1. K. S. L. Al-Badri, Ibn Al-Haitham J. Pure Appl. Sci. **31** (Issue IHSCICONF 2017), 159 (2018).
2. I. Al-Naib, Y. Yang, M. M. Dignam, W. Zhang, and R. Singh, Appl. Phys. Lett. **106**, 011102 (2015).
3. K. J. Vahala, Nature (London, U.K.) **424**, 839 (2003).
4. V. Savinov, A. Tsiatmas, A. R. Buckingham, V. A. Fedotov, P. A. J. de Groot, and N. I. Zheludev, Sci. Rep. **2**, 450 (2012).
5. V. Savinov, K. Delfanazari, V. A. Fedotov, and N. I. Zheludev, Appl. Phys. Lett. **108**, 101107 (2016).
6. V. Savinov, V. A. Fedotov, P. A. J. de Groot, and N. I. Zheludev, Supercond. Sci. Technol. **26**, 084001 (2013).
7. D. Liu, in *Proceedings of the 8th International Symposium on Ultrafast Phenomena and Terahertz Waves* (Optica Publ. Group, 2016), p. IW2A-4.
8. H.-T. Chen, W. J. Padilla, J. M. O. Zide, A. C. Gossard, A. J. Taylor, and R. D. Averitt, Nature (London, U.K.) **444**, 597 (2006).
9. Y. K. Srivastava, M. Manjappa, L. Cong, H. N. S. Krishnamoorthy, V. Savinov, P. Pitchappa, and R. Singh, Adv. Mater. **30**, 1801257 (2018).
10. Y. K. Srivastava, M. Manjappa, H. N. S. Krishnamoorthy, and R. Singh, Adv. Opt. Mater. **4**, 1875 (2016).
11. V. Savinov, V. A. Fedotov, S. M. Anlage, P. A. J. de Groot, and N. I. Zheludev, Phys. Rev. Lett. **109**, 243904 (2012).
12. Y. Wang, Z. Han, Y. Du, and J. Qin, Nanophotonics **10**, 1295 (2021).
13. A. Strikwerda, H. Tao, E. A. Kadlec, K. Fan, W. J. Padilla, X. Zhang, E. A. Shaner, and R. D. Averitt, in *Proceedings of the CLEO:2011—Laser Applications to Photonic Applications* (Optica Publ. Group, 2011), p. QTuD6.
14. J. Mendrok, P. Baron, and Y. Kasai, in *Remote Sensing of Clouds and the Atmosphere XIII,* Proc. SPIE **7107**, 27 (2008).
15. *Handbook of Terahertz Technologies: Devices and Applications,* Ed. by H.-J. Song and T. Nagatsuma (Pan Stanford, Singapore, 2015).
16. Y. Feldman, A. Puzenko, P. Ben Ishai, A. Caduff, and A. J. Agranat, Phys. Rev. Lett. **100**, 128102 (2008).
17. G. S. Park, *Convergence of Terahertz Sciences in Biomedical Systems* (Springer, Dordrecht, 2012).
18. P. L. Richards, J. Appl. Phys. **76**, 1 (1994).
19. W. S. Holland, D. Bintley, E. L. Chapin, A. Chrysostomou, G. R. Davis, J. T. Dempsey, W. D. Duncan, M. Fich, P. Friberg, M. Halpern, and K. D. Irwin, Mon. Not. R. Astron. Soc. **430**, 2513 (2013).
20. R. A. Lewis, J. Phys. D: Appl. Phys. **52**, 433001 (2019).
21. R. Singh and N. Zheludev, Nat. Photon. **8**, 679 (2014).
22. C. Enss, *Cryogenic Particle Detection* (Springer, Berlin, 2005).
23. P. de Bernardis, P. A. R. Ade, J. J. Bock, J. R. Bond, J. Borrill, A. Boscaleri, K. Coble, B. P. Crill, G. De Gasperis, P. C. Farese, and P. G Ferreira, Nature (London, U.K.) **404**, 955 (2000).
24. D. J. Benford and S. Moseley, Nucl. Instrum. Methods Phys. Res., Sect. A **520**, 379 (2004).
25. J. Grant, I. Escorcia-Carranza, C. Li, I. J. H. McCrindle, J. Gough, and D. R. S. Cumming, Laser Photon. Rev. **7**, 1043 (2013).
26. V. Savinov, V. A. Fedotov, P. A. de Groot, and N. I. Zheludev, Supercond. Sci. Technol. **26**, 084001 (2013).
27. A. Noor and Z. Hu, J. Infrared Millim. Terahertz Waves **31**, 791 (2010).
28. F. Alves, L. Pimental, D. Grbovic, and G. Karunasiri, Sci. Rep. **8**, 12466 (2018).
29. A. A. Basharin, V. Chuguevsky, N. Volsky, M. Kafesaki, and E. N. Economou, Phys. Rev. B **95**, 035104 (2017).
30. M. V. Cojocari, K. I. Schegoleva, and A. A. Basharin, Opt. Lett. **42**, 1700 (2017).
31. M. V. Cojocari, V. I. Chuguevsky, N. A. Volsky, and A. A. Basharin, in *Proceedings of the 2019 International Conference on Electromagnetics in Advanced Applications ICEAA* (IEEE, 2019), p. 0696.
32. A. Bhattacharya, R. Sarkar, and G. Kumar, J. Phys. D: Appl. Phys. **54**, 285102 (2021).
33. L. Ma, W. Zheng, J. Li, D. Chen, W. Wang, Y. Liu, Y. Zhou, Y. Yang, Y. Huang, and G. Wen, Results Phys. **24**, 104172 (2021).

34. T. Kaelberer, V. Fedotov, N. Papasimakis, D. Tsai, and N. Zheludev, Science (Washington, DC, U. S.) **330**, 1510 (2010).

35. N. A. Nemkov, A. A. Basharin, and V. A. Fedotov, Phys. Rev. A **98**, 023858 (2018).

36. D. Mattis and J. Bardeen, Phys. Rev. **111**, 412 (1958).

37. V. Merenkov, V. I. Chichkov, and S. V. Shitov, Meas. Tech. **62**, 973 (2020).

38. A. V. Merenkov, T. M. Kim, V. I. Chichkov, S. V. Kalinkin, and S. V. Shitov, Phys. Solid State **64**, 1387 (2022).

39. A. V. Merenkov, V. I. Chichkov, A. V. Ustinov, and S. V. Shitov, J. Phys.: Conf. Ser. **1182**, 012009 (2019).

40. M. E. Gershenson, D. Gong, T. Sato, B. S. Karasik, and A. V. Sergeev, Appl. Phys. Lett. **79**, 2049 (2001).

41. S. V. Shitov, A. A. Kuzmin, M. Merker, V. I. Chichkov, A. V. Merenkov, A. B. Ermakov, A. V. Ustinov, and M. Siegel, IEEE Trans. Appl. Supercond. **27**, 1 (2017).

42. L. S. Kuzmin, A. L. Pankratov, A. V. Gordeeva, V. O. Zbrozhek, V. A. Shamporov, L. S. Revin, A. V. Blagodatkin, S. Masi, and P. de Bernardis, Commun. Phys. **2**, 104 (2019).

43. E. A. Matrozova, A. L. Pankratov, A. V. Gordeeva, A. V. Chiginev, and L. S. Kuzmin, Supercond. Sci. Technol. **32**, 084001 (2019).

44. B. Beiranvand, A. S. Sobolev, M. Y. Larionov, and L. S. Kuzmin, Appl. Sci. **11**, 4459 (2021).